MINERALOGICAL MAGAZINE, VOL. 45, 1982, PP. 139-47

Chemical and morphological variation in tourmalines from the Hub Kapong batholith of peninsular Thailand

D. A. C. MANNING*

Department of Geology, The University, Manchester M13 9PL

ABSTRACT. Electron probe microanalysis of tourmaline from late-stage aplites and mineralized (Sn-W) pegmatites from the Hub Kapong batholith of peninsular Thailand has revealed considerable chemical variation, and has shown that skeletal tourmaline crystals predominate within the pegmatites. The tourmalines show substitution towards the schorl end-member of the schorl–dravite series, as well as substitution towards alkali-free or proton deficient tourmaline. The extent of both substitutions increases (*a*) from aplites to pegmatites and (*b*) from core to rim within a single grain and so is believed to become greater with increasing degrees of differentiation of the aplite-pegmatite system. The development of skeletal crystals within the pegmatites and non-skeletal crystals within the aplites is believed to be due to the different kinetics of crystal growth obtaining within a hydrous, pegmatitic, fluid (viz. heterogeneous nucleation and comparatively rapid crystal growth rates) which in turn arise from differences in the structure of the aplitic magma and pegmatitic fluid. The observed chemical and morphological variation shown by the tourmalines is used to discuss the petrogenesis of the aplites and pegmatites, and associated ore deposits. During differentiation, the volatile content of the aplite magmas increased, leading to water saturation and the separation of a hydrous pegmatitic fluid. After a period of coexistence, possibly in chemical equilibrium, the crystallization of the pegmatites continued once the aplite magma had completely consolidated.

THE geology of peninsular Thailand is dominated by the presence of a belt of granitic intrusions which extends from north Thailand into Malaya. The granite areas are of particular economic importance because of the occurrence of genetically associated tin and tungsten mineralization. In addition to primary pegmatitic and hydrothermal Sn-W deposits, alluvial deposits also occur in close spatial association with pegmatites and late-stage granites.

On a regional scale, the granitic bodies of peninsular Thailand are divided into a western belt of Lower Cretaceous age, which extends from north Thailand following the Thai–Burmese border to Phuket Island, and a central belt of Triassic age represented by plutons in the Hua Hin area and southern peninsular Thailand (Beckinsale *et al.*, 1979). The Triassic granites extend into Malaya as the Main Range Belt (Hutchison, 1977). Detailed geological mapping of the individual components of the granite belts has yet to be completed, but the field relationships of different granite varieties are now known in some detail for the Phuket area and the Hub Kapong batholith (near Hua Hin; Garson *et al.*, 1975; Putthapiban and Suensilpong, 1978). In both areas, although of different ages (Cretaceous and Triassic respectively) the field relationships indicate the early emplacement of biotite (and hornblende)-bearing granites, followed by the later emplacement of muscovite- and tourmaline-bearing granites. In particular, the tourmaline-bearing granite varieties occur as cross-cutting sheets of pegmatite or aplite, which may form composite bodies. Lepidolite pegmatites also occur, in addition to tourmaline-bearing pegmatites, in the Phuket area.

Tourmaline is a complex boro-silicate known to contain tin as a trace element (e.g. Němec, 1973; Power, 1968). It is commonly found in association with tin mineralization throughout the world, which has led to suggestions that the role of boron may be important in the transport and concentration of tin. In order to clarify and assess the significance of the observed association it is necessary to consider the chemical variation shown by tourmaline from tin-mineralized areas, and to attempt to deduce the petrogenetic origin of the tourmaline-bearing rocks. The purpose of this paper is to describe the chemical variation shown by tourmalines from aplites and pegmatites from the Hub Kapong batholith, and to discuss the petrogenetic processes involved in the formation of these late-stage rocks.

* Present address: Centre de Recherches Pétrographiques et Géochimiques, BP 20, 54501 Vandœuvre-lès-Nancy.

Field relations of the samples used in this study. Several examples of tourmaline-bearing aplite and pegmatite were collected from the Hub Kapong area, from localities given by Putthapiban and Suensilpong (1978). Some of the samples were from isolated outcrops of tourmaline-bearing aplite dykes (occasionally bordered by pegmatite) within porphyritic biotite granite (samples 4065, 4069, 4071). Other samples were taken from two separate mineral workings with larger scale, more clear exposure of the field relationships. The first of these, Ban Tha Lao (samples 4050, 4051) consists of a worked-out alluvial deposit, in the floor of which is exposed a reticulate network of thin (2–3 m) inclined dykes of coarse-grained tourmaline aplite. The dykes extend in length for 100–200 m within the area of the workings and were intruded into pelitic sediments. Several of the dykes show the development of thin (up to 20 cm) pegmatitic lenses on the hanging walls. Sn and W minerals are recorded from the aplite–pegmatite dykes and associated quartz veins (Putthapiban and Suensilpong, 1978) and are presumed to have contributed to the superficial deposits which have now been removed. The second major exposure which was studied is the opencast mine of Leu Rot Wong, near Ban Nong Sua. Here an isolated outcrop of aplite with pegmatitic lenses forms a small hill, and is worked as a quarry (approximately 100 m × 20 m, depth 10 m) for cassiterite and wolframite. The contacts between the aplite and country rock are not exposed—the body may be part of a roof complex, or part of a composite flat-lying sheet. The precise occurrence of cassiterite and wolframite is clearly visible at this locality. The cassiterite occurs as a component of some of the pegmatite lenses, as large euhedral crystals (up to 2–3 cm across) enclosing tourmaline. Wolframite occurs mostly within quartz veins up to 20 cm across which cut both pegmatite and aplite. By analogy with similar bodies exposed in north Thailand, the quartz–wolframite veins may be restricted to the aplite–pegmatite body and not enter the country rock. Their formation clearly post-dates the consolidation of the aplite and pegmatite. Samples taken from this locality represent both the aplite (4057, 4063) and the pegmatite (4061, 4062).

The mineralogy of all the samples examined is simple, with quartz, albite and orthoclase as the dominant phases present. Garnet (spessartine–almandine solid solution) occurs in some of the samples (both pegmatite and aplite) and where present, the mica is muscovite which may be primary or secondary after feldspar.

Tourmaline morphology and textural relationships. In most of the samples taken from the aplites and pegmatites of Hub Kapong the tourmalines occur as euhedral or subhedral elongate grains. The pegmatitic tourmalines reach up to 1 cm across in transverse sections, with a length of several centimetres (10 cm or more), although they are frequently fractured. Tourmalines from the aplites have similar proportions, but with a maximum length of the order of 5 mm. Transverse sections of pegmatitic tourmaline are frequently cored with either quartz or alkali feldspar—this feature can clearly be seen in hand specimen as well as in thin sections, and is very occasionally seen in thin sections of aplitic tourmalines. In thin section the euhedral tourmaline grains show concentric colour zoning, as illustrated by the sketch sections given in fig. 1. Two different types of morphology are distinguished. In fig. 1*a*, the transverse sections show concentric zoning from a pale-khaki core via a khaki-green body to a pale-khaki rim. In this case, the pale-khaki cores and rims differ in chemical composition (see later). The second morphological type (fig. 1*b*) shows similar concentric zoning, but some sections have a core of quartz or alkali feldspar in the form of a negative tourmaline crystal. The pale-khaki cores in this case have similar chemical composition to the pale-khaki rims, and so are considered to be the *inner rims* of skeletal crystals. It should be noted that the transverse sections of types A(1,2) and B(2,3) cannot be distinguished without analysis of the different zones of the section.

Although most of the samples examined gave euhedral transverse or longitudinal sections as described above, some aplites were found to contain anhedral grains with irregular colour zoning. Blue-coloured tourmaline was occasionally observed in thin section, but was scarce, occurring as isolated anhedral grains or patches of blue coloration in khaki-green regions.

Analytical data. Partial chemical analyses of the tourmalines have been determined using the electron microprobe (Cambridge Geoscan III with Link Systems Ltd. energy dispersive analytical system). The electron beam size was approximately 5 μm and the beam intensity was adjusted to give a total $100 \pm 0.5\%$ on analysis of albite, which is present in all the tourmaline-bearing material studied. Individual analyses have been grouped according to the colour of the grain at the point of analysis and the position of the point of analysis within the grain, using the categories given above and illustrated in fig. 1. The analyses are summarized in Table I, which gives the mean value of the analyses for a given sample, and the 2σ variation for the combined analyses within each category. The analytical precision, estimated by Dunham and Wilkinson (1978), is between 0.22 and 0.36 wt. % for 10 wt. % oxide, 0.52 % for 50 wt. % SiO_2.

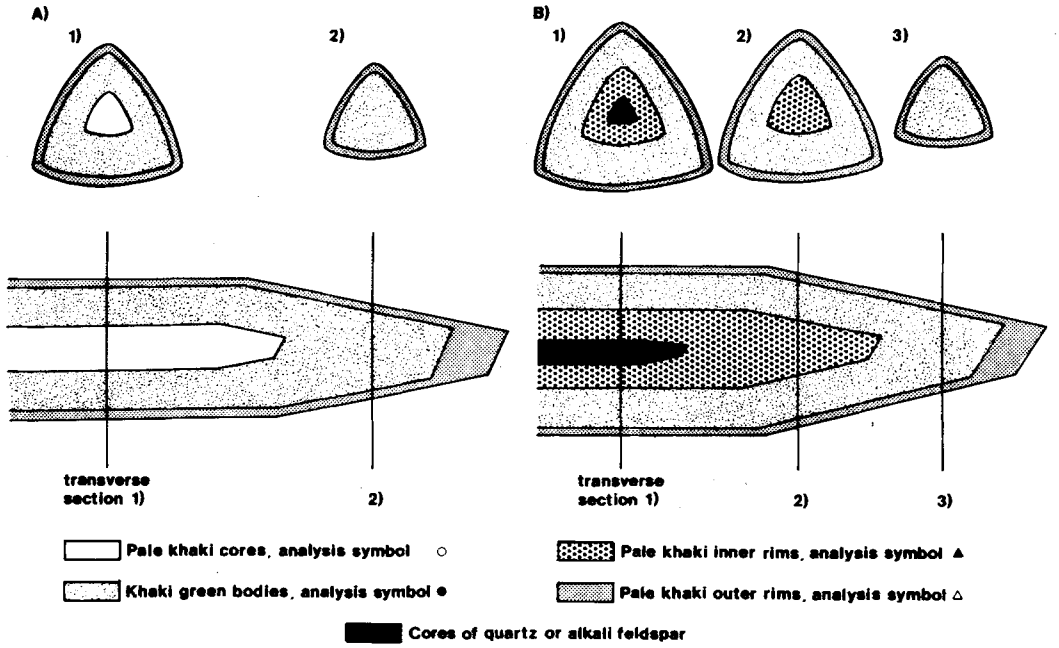

FIG. 1. Schematic diagrams showing transverse and longitudinal sections of (A) non-skeletal and (B) skeletal tourmaline crystals from Hub Kapong.

Thus the 2σ values given in Table I show that there are significant differences between each of the three major categories. In general, the khaki-green areas have a higher Ti content than the less strongly coloured pale-khaki areas (although subjective, this is the only case where the intensity of the colour observed and element concentration may be correlated). The blue bodies were only observed for a single sample, 4069, and do not differ significantly in composition from the khaki-green bodies. The pale-khaki areas can be subdivided into two categories—Mg-rich cores and Mg-poor rims (including the inner rims of skeletal crystals). Mn contents are very variable, reaching 1.04% MnO in some of the pale-khaki coloured Mg-poor rims. (NB the value for MnO of 2.00% in sample 4065*b* is exceptionally high, and was found for a single grain.) The Fe and Mg contents are also very variable reflecting extensive solid solution between schorl and dravite end-members, $NaFe_3Al_6(BO_3)_3Si_6O_{18}(OH)_4$ and $NaMg_3Al_6(BO_3)_3Si_6O_{18}(OH)_4$ respectively.

In order to clarify the relationships between the different populations, individual analyses have been plotted in ternary TiO_2–MgO–(FeO + MnO) diagrams (fig. 2). The diagrams clearly show an overall compositional trend from high-Mg pale-khaki cores to khaki-green bodies to low-Mg pale-khaki inner and outer rims, with the most schorl-rich compositions given by the rims of tourmalines from pegmatites. The tourmalines from the aplites show a large part of the overall trend (even within single crystals), but rarely does a given sample show the entire trend. An exception to this is the material from the composite aplite–pegmatite sheets of Ban Tha Lao. The compositional trend shown by tourmaline from aplite from this locality (4050; fig. 2*a*) extends from pale-khaki cores (high-Mg) via khaki-green bodies to pale-khaki rims (low-Mg) and continues, with overlap, for the pegmatitic tourmalines (4051; fig. 2*b*) from khaki bodies to pale-khaki (low-Mg) inner and outer rims. Similar trends are shown by tourmalines from aplite (4057, 4063; fig. 2*f*) and pegmatite (4061, 4062; fig. 2*g*, *h*) from the composite body of Ban Nong Sua.

Atomic proportions have been calculated to 31 (O,OH) from the partial analyses assuming (1) complete occupancy of the F–OH site by 4OH, (2) the presence of three B atoms per formula unit, and (3) that Fe is totally present as Fe^{2+}. These assumptions are unlikely to be true because some F may be present (although this was not determined) and some of the Fe will be present as Fe^{3+} (which cannot be determined by electron-microprobe analysis). The calculated proportions (Table I) show that the general formula for the

TABLE I. *Electron-microprobe analyses, and atomic proportions, for tourmalines from Hub Kapong*

	Khaki-green bodies											Blue bodies	Pale-khaki cores			Pale-khaki inner and outer rims							
	4050	4051	4057	4061	4062	4063	4065		4069	4071	2σ	4069	4050	4069	2σ	4050	4051	4057	4061	4062	4069	4071	2σ
							(a)	(b)															
Na_2O	2.26	1.90	2.14	1.68	1.72	2.05	2.09	2.14	1.82	1.82	0.40	1.80	1.75	1.37	0.31	2.44	1.87	2.32	1.32	1.35	1.50	1.81	0.36
MgO	2.87	1.41	2.49	1.29	0.43	2.21	2.80	0.30	1.91	1.05	0.97	1.59	2.89	2.14	0.50	1.52	0.82	0.78	0.92	0.30[1]	0.46[1]	0.53	0.30
Al_2O_3	32.90	32.05	33.46	35.11	34.64	34.55	34.02	36.61	35.36	34.90	1.11	32.75	34.65	36.32	0.63	32.17	32.98	32.72	35.62	35.46	36.18	35.58	1.02
SiO_2	34.99	34.93	34.72	35.24	35.24	36.31	36.15	35.94	36.11	35.52	0.80	35.52	34.20	36.82	0.48	34.67	35.12	34.86	36.25	36.21	36.66	35.94	0.64
CaO	0.43	0.46	0.39[1]	0.41	0.25	0.32	0.38	0.35	0.19	0.20	0.19	0.73	0.18[1]	0.10[1]	0.08	0.20	0.32	0.46	0.14[1]	0.12[2]	n.d.	0.14	0.09
TiO_2	1.00	0.98	0.87	1.14	0.91	0.57	0.69	0.59	0.69	0.88	0.33	0.85	0.32	0.35	0.17	0.75	0.36	0.53[1]	0.45	0.30	0.29	0.46	0.29
MnO	0.33[1]	0.28[1]	0.36	0.19[1]	0.40	0.23[1]	0.63	2.00	0.29	0.27	0.22	0.39	0.21[2]	0.25[2]	0.08	0.73	0.31	0.48	0.20[2]	0.41	0.49	0.33[2]	0.21
FeO	13.64	14.98	13.14	13.34	14.64	13.31	10.63	9.43	12.90	14.05	1.46	14.57	12.00	11.69	0.41	15.14	15.04	16.55	13.41	14.03	14.15	14.38	0.95
Total	88.42	86.99	87.57	88.40	88.23	89.55	87.39	87.36	89.27	88.69		88.20	85.90	88.84		87.62	86.82	88.70	88.31	88.18	89.73	89.17	
Na	0.724	0.622	0.690	0.534	0.551	0.643	0.664	0.678	0.570	0.578		0.579	0.567	0.425		0.797	0.611	0.752	0.417	0.429	0.468	0.571	
Mg	0.707	0.355	0.617	0.315	0.106	0.533	0.684	0.073	0.460	0.256		0.393	0.720	0.511		0.382	0.206	0.194	0.224	0.073	0.110	0.129	
Al	6.408	6.374	6.555	6.778	6.747	6.585	6.570	7.049	6.734	6.737		6.406	6.827	6.855		6.386	6.554	6.449	6.842	6.848	6.868	6.828	
Si	5.782	5.894	5.771	5.772	5.824	5.872	5.924	5.872	5.835	5.818		5.895	5.718	5.897		5.839	5.922	5.829	5.908	5.933	5.905	5.852	
Ca	0.076	0.083	0.070	0.072	0.044	0.055	0.067	0.061	0.033	0.035		0.130	0.032	0.017		0.036	0.058	0.082	0.024	0.021		0.024	
Ti	0.124	0.124	0.109	0.140	0.113	0.069	0.085	0.073	0.084	0.108		0.106	0.040	0.042		0.095	0.046	0.067	0.055	0.037	0.035	0.056	
Mn	0.046	0.040	0.051	0.026	0.056	0.032	0.087	0.277	0.040	0.038		0.055	0.030	0.034		0.104	0.044	0.068	0.028	0.057	0.067	0.046	
Fe	1.885	2.114	1.827	1.827	2.023	1.800	1.457	1.288	1.743	1.925		2.022	1.678	1.656		2.133	2.121	2.314	1.828	1.923	1.906	1.958	
n	41 ([1]33)	11 ([1]10)	22 ([1]21)	13 ([1]12)	14 ([1]13)	10 ([1]8)	17	3	14	15 ([1]13)		4	27 ([1]26) ([2]12)	5 ([1]3) ([2]4)		16	19	7 ([1]5)	15 ([1]13) ([2]14)	11 ([1]10) ([2]7)	7 ([1]6)	15 ([1]6) ([2]14)	

4050 aplite, Ban Tha Lao; 4051 pegmatite, Ban Tha Lao; 4057, 4063 aplite, Ban Nong Sua; 4061, 4062 pegmatite, Ban Nong Sua; 4065, 4069, 4071 aplites, various localities. n.d. = below detection limit; n = no. of analyses.

schorl–dravite series, $R^+R_3^{2+}R_6^{3+}(BO_3)_3Si_6O_{18}(OH)_4$, is not obtained, as there is a deficiency in R^+ (Na+2Ca) and R^{2+} (Mg+Mn+Fe) and an excess of R^{3+} (Al+4/3Ti). These discrepancies from the general formula may be due to the effect of two coupled substitutions elucidated by Foit and Rosenberg (1977):

$$(OH)^- + R^{2+} \rightleftharpoons R^{3+} + O^{2-} \quad (1)$$

$$R^+ + R^{2+} \rightleftharpoons R^{3+} + \square \quad (2)$$

Substitution (1) leads to a proton-deficient end member, $R^+R_3^{3+}R_6^{3+}(BO_3)_3Si_6O_{18}O_3(OH)$, and substitution (2) leads to an alkali-free end member, $\square(R_2^{2+}R^{3+})R_6^{3+}(BO_3)_3Si_6O_{18}(OH)_4$. Clearly the full extent and relative importance of either substitution cannot be evaluated from the partial electron-microprobe analyses. However, it can be demonstrated that the analyses show the existence of considerable coupled substitution. The analyses for samples 4050 and 4051, which show the overall extent of schorl–dravite solid solution, are plotted as $R^+ + R^{2+}$ *vs.* R^{3+} in fig. 3. The plots extend

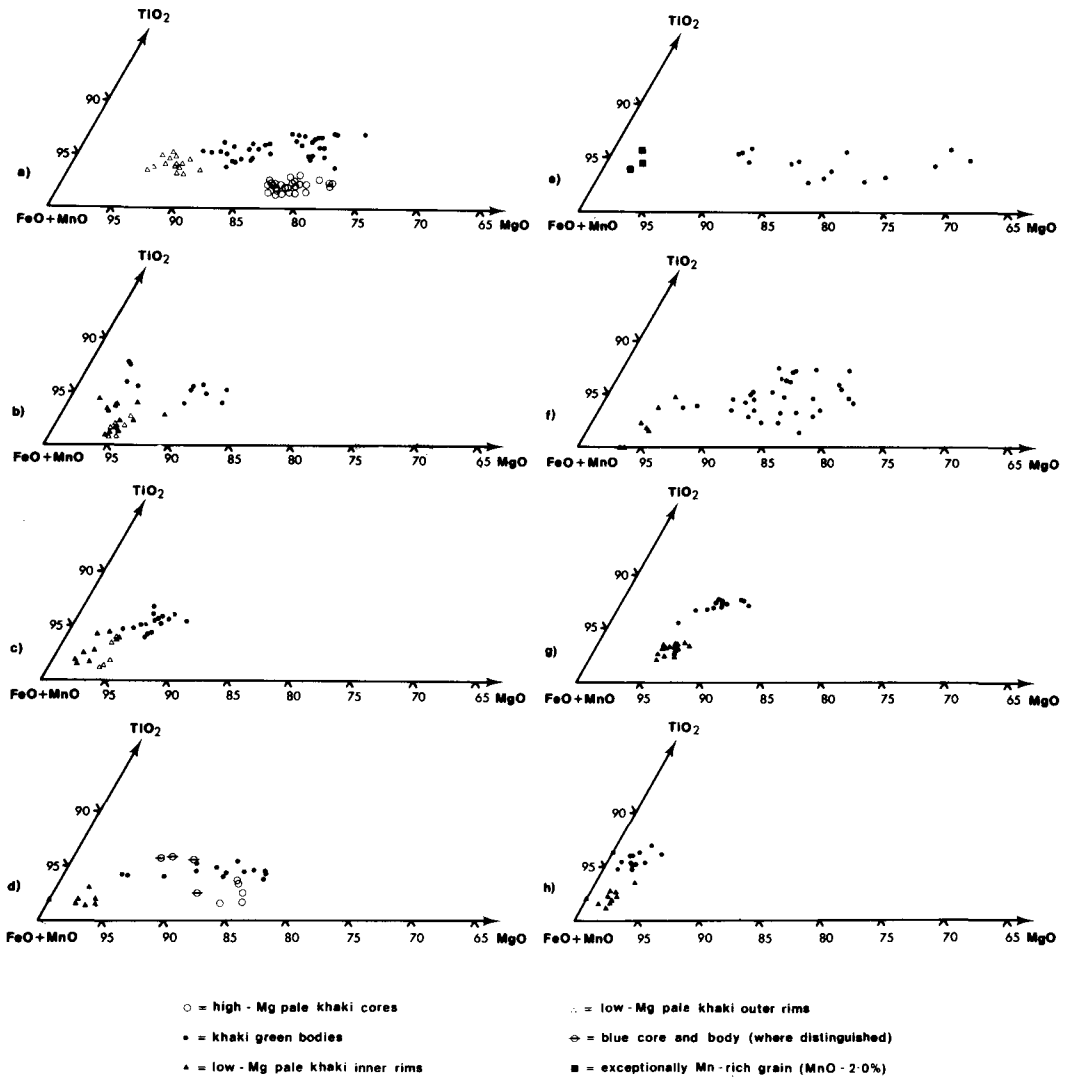

FIG. 2. Plots in $MgO–TiO_2–(FeO+MnO)$ for tourmalines from the Hub Kapong batholith. (*a*, *b*) are for aplite and pegmatite 4050, 4051 respectively; (*c*, *d*, *e*) are for aplites 4071, 4069, 4065 respectively; (*f*) is for aplite (4057 and 4063 combined), (*g*, *h*) are for pegmatites 4061, 4062. Sample numbers are as in Table I.

well away from the schorl–dravite end member towards either the alkali-free or the proton-deficient hypothetical end members, with greater degrees of substitution shown by the rims and skeletal cores than the bodies of the tourmalines.

Discussion

Both the chemical variation shown by the tourmalines from Hub Kapong and the presence in some cases of skeletal crystals as revealed by

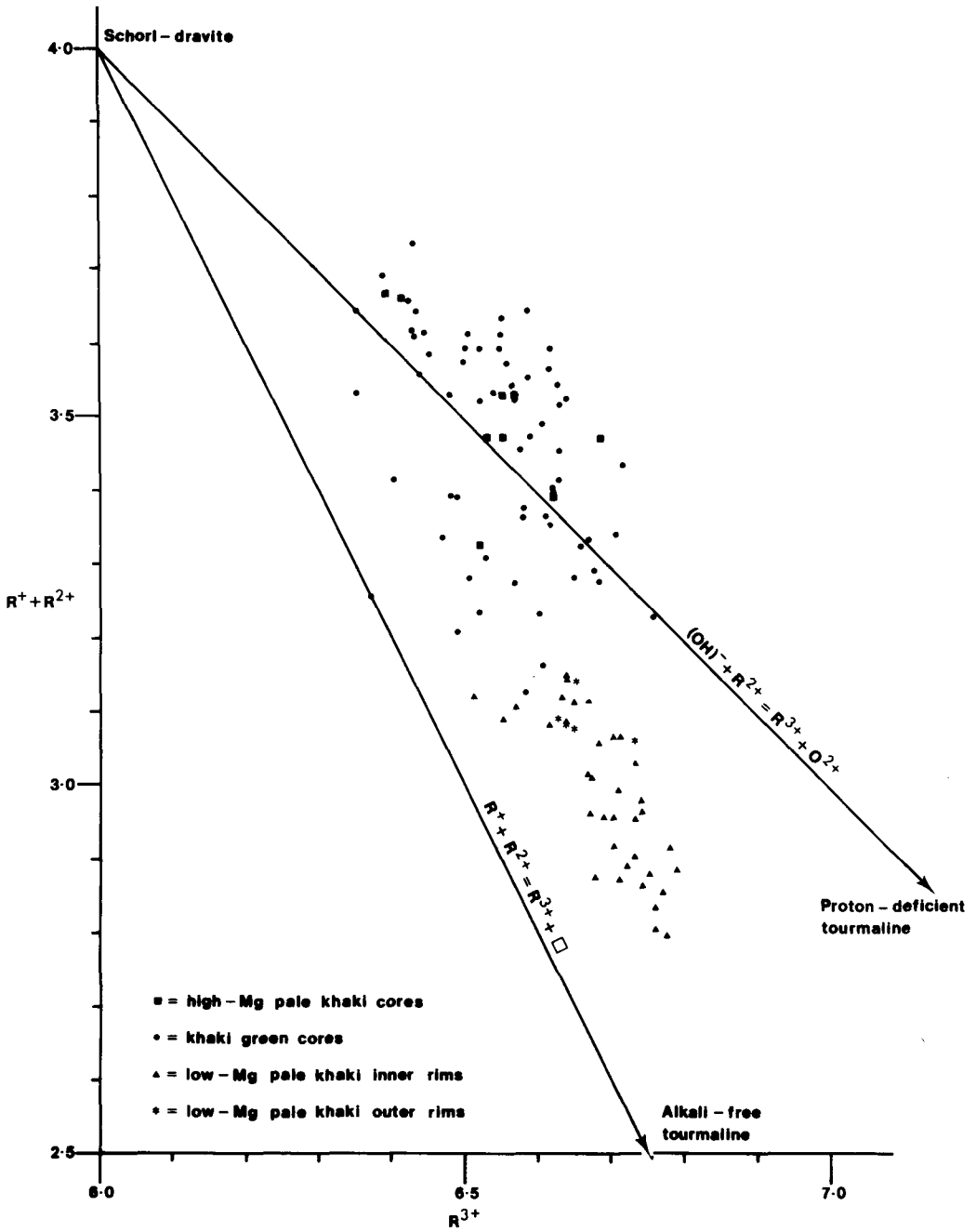

FIG. 3. Plot of $R^+ + R^{2+}$ *vs.* R^{3+} for tourmalines from aplite and pegmatite from Ban Tha Lao (samples 4050, 4051 combined).

electron microprobe analysis may be used to discuss the petrogenesis of the tourmaline-bearing aplites and pegmatites, and the associated pegmatitic ore deposits.

Chemical Variation. A number of major and trace element determinations for tourmalines of the schorl–dravite series from different petrological environments have previously been carried out (e.g. Power, 1968; Lister, 1979; Neiva, 1974). Most previous studies involved complete analyses of tourmaline separates, but Lister (1979) carried out an electron microprobe study of pegmatitic tourmalines from SW England. In order to compare the results of these studies with those of the present investigation, published analyses have been recalculated and plotted (with Fe_2O_3 recalculated as FeO) in the ternary diagram TiO_2–MgO–(FeO + MnO) (fig. 4). The data of Power (1968) for tourmalines from SW England (fig. 4*a*) show a trend from relatively Mg-rich tourmaline in granitic rocks to a composition close to schorl in tourmaline–quartz rock and topaz–quartz–tourmaline rock. This sequence is interpreted by Power as reflecting a trend towards the schorl end member during magmatic differentiation. The data of Lister (1979) are consistent with this interpretation (fig. 4*b*). The tourmalines from pegmatitic lenses within biotite granite (the earliest major granite variety present in SW England) from Tregarden are the most dravite-rich. Those from roof pegmatites associated with lithium-mica granite (Megiliggar Rocks), which are believed to be late differentiates, are the most schorl-rich. Intermediate tourmaline compositions are given by other pegmatites with less certain age relationships (Cape Cornwall, Goonbarrow). In addition, these analyses show, within a given category, schorl enrichment in skeletal crystals. Tourmalines from Portugal also show a trend of schorl enrichment in a sequence from biotite granite to later aplite and pegmatite (fig. 4*c*; Neiva, 1974).

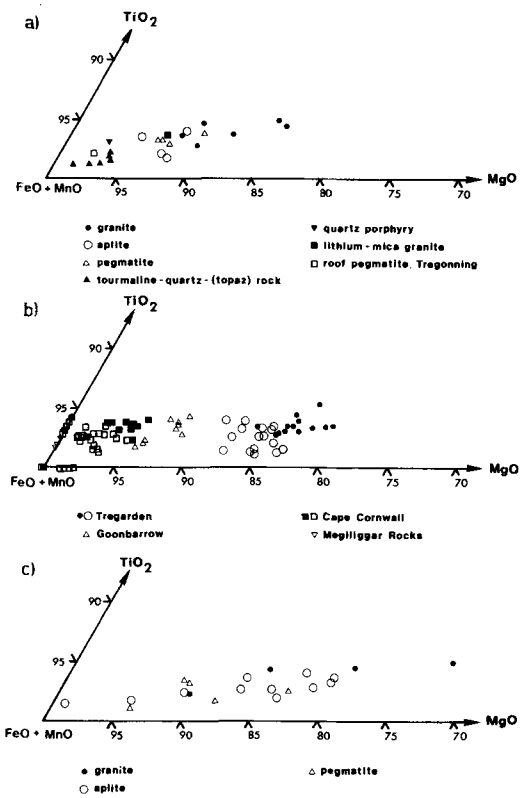

FIG. 4. Plots in MgO–TiO_2–(FeO + MnO) for published tourmaline analyses. (*a*) bulk analyses of tourmalines from SW England; Power (1968). (*b*) electron-microprobe analyses, pegmatitic tourmalines, Cornwall; Lister (1979). Open symbols indicate skeletal crystals. (*c*) bulk analyses of tourmalines from Portugal; Neiva (1974).

The extent of schorl–dravite solid solution shown by the tourmalines from Hub Kapong is similar to that shown by tourmalines from SW England and Portugal (fig. 4). Of particular interest is the variation in composition shown by single grains within certain samples, which show extreme zoning (e.g. fig. 2*a*). Overall, there is a continuous sequence of variation in the degree of schorl–dravite solid solution from dravite-rich cores for tourmalines from aplites to schorl-rich rims for tourmalines from the pegmatites. This is consistent with an increase in the schorl content as crystallization proceeds. The compositional variation shown by pegmatitic tourmaline and aplitic tourmaline in some cases overlaps (fig. 2*a*, *b*, *f*, *g*, *h*). This similarity suggests that both crystallized at the same time, from coexisting pegmatitic fluid and aplite magma which were in chemical equilibrium with respect to the components which make up tourmaline.

The physicochemical conditions governing the extent of substitution towards alkali-free or proton-deficient tourmaline end members are as yet unknown. Rosenberg and Foit (1979) have synthesized alkali-free tourmaline, and note that the alkali site occupancy by Mg^{2+}, and Al content, are higher, while the proton content is lower, for tourmaline synthesized at lower temperatures. The extent of substitution towards alkali-free or proton-deficient tourmaline may become greater with decreasing temperature of crystallization (or effectively with increasing degree of differentiation). This possibility is suggested by the tourmalines of Hub Kapong, with the rims of a given crystal showing more extensive substitution of this type than the earlier cores (fig. 3). The observed substitution of Al for R^{2+} is also consistent with the

preference shown by tourmaline for high field strength cations (Foit and Rosenberg, 1979).

A major disadvantage of using electron-microprobe analysis in a study of tourmaline compositional variation is that the analyses are partial and do not include trace elements, boron, or water. The trace element content of tourmalines can be of considerable interest as tourmaline is often the only ferromagnesian mineral present in late-stage granitic rocks. In particular, Power (1968) notes that the tin content of tourmalines from SW England increases with the degree of differentiation, and Němec (1973) records that the tin content of tourmaline from areas of tin mineralization is greater than that from non-mineralized areas. However, the considerable variation in major element composition within single grains of tourmaline, which is revealed by electron-microprobe analysis, suggests that there may also be substantial variation in the trace element content. This possibility should be borne in mind in a study of the trace element content of tourmalines as bulk analyses of tourmaline separates will not reveal the full extent of trace element variation for a given sample.

The origin of skeletal tourmaline crystals. The tourmalines from the pegmatites and some aplites from Hub Kapong show evidence for skeletal growth, with the presence of quartz and feldspar cores and compositional similarity between the inner and outer rims. Quartz-cored tourmalines have been noted before, from SW England (Lister, 1979) and Nigeria (McCurry, 1971). Whereas McCurry (1971) suggests that the quartz-cored tourmalines from Nigeria were formed by the preferential replacement of tourmaline cores by quartz, Lister (1979) considers that the quartz-cored tourmalines from SW England grew as skeletal crystals which were later infilled by quartz.

The growth of skeletal crystals in systems of geological interest has been studied by many workers, and is reviewed by Dowty (1980) and Lofgren (1980). Briefly summarized, the conditions favouring skeletal growth are (1) a high degree of supersaturation of the medium of growth (as caused by increased degrees of supercooling below the liquidus); (2) high crystal growth rates; and (3) low diffusion rates. Knowledge of the effects of varying these parameters enables the physical conditions for growth of a given mineral to be compared from one environment to another (for example in comparison of olivine morphology in plutonic, hypabyssal and volcanic rocks of roughly similar composition). The physical conditions controlling the growth of skeletal tourmaline crystals will be as outlined above (Lister, 1979), but there will be significant differences in their relative importance arising as a consequence of growth from a pegmatitic fluid rather than a silicate magma. These differences arise from the nature of the internal structure of the water-dominated pegmatitic fluids, in which the network-forming elements Si and Al are more likely to be present as low-order polymers (monomers or possibly dimers) than as high-order polymeric networks (as in aluminosilicate melts) because of the known disruptive effect on such networks by volatiles such as H_2O and F (Burnham, 1979; Manning *et al.*, 1980). The first major difference is that nucleation of crystals from a pegmatitic fluid is predominantly heterogeneous, using pre-existing solid-fluid interfaces, whereas nucleation from a melt is believed to be predominantly homogeneous. This is clearly illustrated by the growth of crystals from the walls and internal surfaces of pegmatite bodies, and is a consequence of the relatively low probability that random motion of the network-forming elements will produce large enough nuclei to enable silicate crystal growth to begin within the bulk of the pegmatitic fluid. Secondly, the very much lower viscosity of pegmatitic fluids (10^{-3}–10^{-4} poise, cf. 10^{6}–10^{7} poise for hydrous granite magmas; Jahns and Burnham, 1969) will lead to very much greater crystal growth rates and diffusion rates than obtained for a hydrous granite magma. Consequently, in coexisting aplite magma and pegmatitic fluids at chemical equilibrium, and at the same temperature and pressure, the degree of supersaturation with respect to a given mineral species may be the same for both the silicate and hydrous phase, but differences in crystal morphology will arise as a consequence of the different physical properties of each phase. The heterogeneous nucleation kinetics and high crystal growth rates obtaining for the pegmatitic fluid will possibly be the most significant factors controlling crystal morphology, and may therefore be responsible for the growth of skeletal crystals within the pegmatite.

Skeletal tourmaline crystals also occur within aplites from composite aplite–pegmatite bodies (4057, 4063, 4069, 4071; fig. 2*c*, *d*, *f*). Such crystals are rare, and poorly developed, compared with the predominance of euhedral skeletal tourmaline grains within the pegmatites. The presence of skeletal tourmaline within the aplites suggests that conditions favouring rapid crystal growth (viz. a reduction in melt viscosity and disruption of melt structure) were obtained within residual melts as differentiation proceeded. However, the difference in form and occurrence of skeletal grains within aplites compared with pegmatites is consistent with markedly different conditions of tourmaline growth in either medium.

Petrogenetic implications. The observed chemical variation and changes in crystal morphology

shown by the tourmalines from aplites and pegmatites from Hub Kapong may be used to trace the evolution of the tourmaline-bearing rocks. The earliest of these are aplites, with relatively draviterich, Ti-poor tourmaline, which gave, as crystallization proceeded, Ti-rich and increasingly schorl-rich tourmaline. The volatile content of the residual melts increased with differentiation, leading to water-saturation of the melts and separation of a hydrous pegmatitic fluid. The concomitant changes in physical properties of the aplite magma during differentiation and volatile enrichment may have led to the limited initial development of skeletal tourmaline crystals within the aplite. However, the major differences in structure and hence crystallization kinetics between the pegmatitic fluid and aplite melt were probably responsible for the predominance of euhedral skeletal crystals within the pegmatites. Tourmaline of the same composition crystallized from both the pegmatites and aplites together, suggesting that a certain degree of chemical equilibrium obtained between the two phases during their coexistence. After consolidation of the aplite, tourmaline continued to crystallize from the pegmatitic fluids, becoming increasingly schorl-rich. The overall trend of schorl enrichment was also accompanied by substitution towards alkali-free or proton-deficient tourmaline.

If the observations have been correctly interpreted, then the presence is demonstrated of the critical stage of coexistence of pegmatitic fluids with residual aplite magma. At this stage partitioning of metals, particularly tin, from residual melts to the hydrous pegmatitic fluid may have taken place. The pegmatites of Hub Kapong may owe their high tin content, sufficient to enable cassiterite to crystallize, to this period of partitioning. W may also have been partitioned into the pegmatitic fluid; however, the occurrence of tungsten minerals in quartz veins cutting the pegmatites indicates that the W mineralization originated from hydrothermal events which followed pegmatite formation. The behaviour of W may therefore have been rather more complex than that of Sn.

Acknowledgements. I am grateful to the Royal Thai Department of Mineral Resources for their kind hospitality and assistance in the field. I am particularly grateful to Prinya Putthapiban, with whom I was able to collect the samples, and to Dr Sanarm Suensilpong. I would also like to thank Professor P. E. Rosenberg and Dr C. M. B. Henderson for their help in improving the manuscript. This work was carried out with the financial support of the NERC, in the form of a research fellowship.

REFERENCES

Beckinsale, R. D., Suensilpong, S., Nakapadungrat, S., and Walsh, J. N. (1979) *J. Geol. Soc. London*, **136**, 529–40.

Burnham, C. W. (1979) In *The Evolution of Igneous Rocks, 50th Anniversary Perspectives* (Yoder, H. S., ed.), Princeton University Press.

Dowty, E. (1980) In *Physics of Magmatic Processes* (Hargraves, R. B., ed.), Princeton University Press.

Dunham, A. C., and Wilkinson, F. C. F. (1978) *X-ray Spectrom.* **2**, 50–6.

Foit, F. F., and Rosenberg, P. E. (1977) *Contrib. Mineral. Petrol.* **62**, 109–27.

——— (1979) *Am. Mineral.* **64**, 788–98.

Garson, M. S., Young, B., Mitchell, A. H. G., and Tait, B. A. R. (1975) *Overseas Mem. Inst. Geol. Sci. London*, **1**.

Hutchison, C. S. (1977) *Bull. Geol. Soc. Malaysia*, **9**, 187–207.

Jahns, R. H., and Burnham, C. W. (1969) *Econ. Geol.* **64**, 843–64.

Lister, C. J. (1979) *Proc. Ussher Soc.* **4**, 402–18.

Lofgren, G. (1980) In *Physics of Magmatic Processes* (Hargraves, R. B., ed.), Princeton University Press.

McCurry, P. (1971) *Am. Mineral.* **36**, 1078–89.

Manning, D. A. C., Hamilton, D. L., Henderson, C. M. B., and Dempsey, M. J. (1980) *Contrib. Mineral. Petrol.* **75**, 257–62.

Neiva, A. M. R. (1974) *Geochim. Cosmochim. Acta*, **38**, 1307–17.

Němec, D. (1973) *Neues Jahrb. Mineral., Monatsh.*, 58–63.

Power, G. M. (1968) *Mineral, Mag.* **36**, 1078–89.

Putthapiban, P., and Suensilpong, S. (1978) *J. Geol. Soc. Thailand*, **3**, M1, 1–22.

Rosenberg, P. E., and Foit, F. F. (1979) *Am. Mineral.* **64**, 180–6.